1.—AN X-RAY STUDY OF WEST AUSTRALIAN BERYL.

By

K. NORRISH, B.Sc. HONS.
(University of Western Australia.)

Read : 12th August, 1947.

INTRODUCTION.

In recent years beryl has increased in importance in this State, mainly because of the use of beryllium in copper, acid resistant and other alloys. The mineral beryl, $Be_3\ Al_2\ Si_6\ O_{18}$, is the main source of beryllium.

Beryl is found in workable quantities in many areas of Western Australia. A study of Western Australian beryls is being made at the Government Chemical Laboratories and at the Geology Department of the University. The X-ray investigations described here were carried out in conjunction with these other studies.

The sample taken for X-ray investigation was from Yinnietharra (31°30′S. 121°35′E.) where one of the main occurrences of workable beryl in Western Australia is found (1).

EXPERIMENTAL.

Preliminary Observations.

The crystal studied was a clear transparent pale green of almost gem quality. The sample had no crystal faces or cleavage planes ; the surfaces consisted of concoidal fractures. It was brittle and hard.

The density was determined accurately by two methods. The first determination was made using a pycnometer while the second consisted in weighing a crystal in and out of water. In the second method, an empirical correction was made for the effect of the surface tension of water on the wire holding the crystal. In both cases corrections were applied to eliminate buoyancy and temperature errors. The methods used are described in the Dictionary of Applied Physics (2). The values found for the density were 2.713 and 2.715 gm. $cm.^{-3}$

Under polarised light the crystal was found to be optically uniaxial. The refractive indices were supplied by Dr. R. T. Prider of the Department of Geology of the University of Western Australia, as follows :—

For the ordinary ray (vibrations parallel to the lateral axes)	$\omega = 1.5825$
For the extraordinary ray (vibrations parallel to the optic axis)	$\varepsilon = 1.5761$

Chemical Analysis.

The chemical analysis was carried out by Mr. H. P. Rowledge, Deputy Government Mineralogist, Government Chemical Laboratories, and appears in Table 1. The theoretical percentages on the basis of $Be_3\ Al_2\ Si_6\ O_{18}$ are also shown.

TABLE 1.

Chemical Analysis of Beryl.

	Actual Percentage.	Theoretical Percentage.
SiO_2	64 .85	67 .06
Al_2O_3	17 .52	18 .97
Fe_2O_3	0 .37	....
MnO	0 .01	....
MgO	0 .14	....
CaO	*Nil*	....
BeO	13 .15	13 .97
Li_2O	0 .52	....
Na_2O	0 .94	....
K_2O	0 .16	....
$(Rb\ Cs)_2O$	0 .08	....
H_2O (given off above 105C.)	2 .19	....
TiO_2	*Nil*	....
P_2O_5	*Nil*	....
Cr_2O_3	*Nil*	....
F	*Nil*	....
Cl	*Nil*	....
Total	99 .93	....

Impurities occur in the crystal lattice by replacing ions of a similar radius. The structural formula is shown calculated in Table 2. It was calculated on the basis of 18 oxygen atoms per molecule, that is, it was assumed that the silicon tetrahedral structure is unaltered by replacements. The water is assumed to be present as OH^- ions replacing oxygen ions.

In the first column of Table 2 is listed the metals present, in order of increasing ionic radius. The ionic radii, taken from Evans (3), are shown in

TABLE 2.

Calculation of Structural Formula of Beryl from the Chemical Analysis.

Metals Present.	Radius of Metal Ion.	Weight.	Molecular Weight.	Molecular Proportions.	Number of Oxygen Atoms.	Number of Metal Atoms on the basis of 18 (O, OH).		
		%						
BeO	0 .34	13 .15	25 .02	0 .5260	0 .5257	2 .809		
SiO_2	0 .39	64 .85	60 .06	1 .0797	2 .1600	5 .772	0 .191	3
							5 .581	
Al_2O_3	0 .57	17 .52	101 .94	0 .1720	0 .5160	1 .840	0 .419	6
							1 .421	
Fe_2O_3	0 .67	0 .37	159 .70	0 .0023	0 .0069	0 .025		
MgO	0 .78	0 .14	40 .32	0 .0035	0 .0035	0 .019		
Li_2O	0 .78	0 .52	29 .88	0 .0174	0 .0174	0 .186		
MnO	0 .91	0 .01	70 .93	0 .0001	0 .0001	0 .001		1 .836
Na_2O	0 .98	0 .94	61 .99	0 .0152	0 .0152	0 .162		
K_2O	1 .33	0 .16	94 .19	0 .0017	0 .0017	0 .018		
$(Rb\ Cs)_2O$	1 .57 (average)	0 .08	234 (average)	0 .0003	0 .0003	0 .004		
H_2O	....	2 .19	18 .02	0 .1215	0 .1215	1 .299		
	....	....	....	....	3 .3683			

Structural formula is $(Be, Si)_{3.00}\ (Si, Al)_{6.00}\ (Al, Fe, etc.)_{1.836}\ O_{18}$.

Molecular weight calculated from the structural formula is 534 .3 atomic weight units.

Column 2, with the percentages by weight in the next column. The molecular proportions of the metals (Column 5) were obtained by dividing their percentage weights (Column 3) by their molecular weights (Column 4). From the molecular proportions the total number of oxygen atoms are found (Column 6) and then the number of metal atoms per molecule are determined on the basis of 18 oxygen atoms. These last figures were found by dividing the number of oxygen atoms (3.368) into 18 and using this factor to multiply the figures in Column 5.

In some of the samples of beryl, water was present as minute inclusions (in tubes parallel to the *c* axis) but there was no evidence of the water being present as inclusions in the sample under consideration.

Optimum Thickness of Beryl for Use with X-rays.

It may be shown (4) that the optimum thickness of a sample for use with X-rays is $\frac{2}{\mu}$ where μ is the linear absorption coefficient of the sample for the X-rays being used. From the mass absorption coefficients for Be, O, Al and Si supplied in the Handbook of Chemistry and Physics (5), the mass absorption coefficient for beryl is calculated to be 32.45 cm.^{2} gm.$^{-1}$, for CuKα radiation. This gives for the linear absorption coefficient 88 cm.$^{-1}$ and for the optimum thickness of beryl 0.2 mm.

Laue Diffraction Patterns.

To obtain Laue diffraction patterns a suitable crystal is set stationary with a crystal axis parallel to the X-ray beam. Having a crystal axis parallel to the X-ray beam simplifies the interpretation considerably. General radiation is used.

As mentioned earlier, beryl has a single optic axis ; this defines and is identical with the *c* axis. Using a geological microscope and a large crystal, the *c* axis was found and a plane perpendicular to this direction was ground and polished. As the crystal was too small to handle comfortably, it was ground after being cemented into celluloid. The grinding could only be carried out to within several degrees of the required direction. After polishiug the crystal was broken and a small piece, having one surface polished, was selected. This was then ground, preserving the polished surface, until the crystal was of the required dimensions (approximately 0.3 x 0.3 x 1.5 mm.).

The crystal fragment was attached, using wax, to the needle point of the two circle goniometer. Previously the goniometer and spectrograph had been adjusted by optical methods using the telescope and collimator supplied with the Hilger unit.

To set the *c* axis parallel to the X-ray beam, a ray of light was passed down the X-ray collimating system and the crystal was adjusted until the polished surface reflected the light back through the collimator.

The crystal was then irradiated with general radiation, from a Coolidge tube operated at 60 kilo-volts and 5 milli-amperes. Under these conditions, using intensifying screens on both sides of the film, about four hours were required to obtain a well-exposed film but a half an hour's exposure was enough for preliminary patterns. The film was mounted in a flat container. The first pattern (see text fig. 9) was not symmetrical, indicating that the *c* axis was not parallel to the X-ray beam.

Adjustments and exposures were made until the crystal was set correctly to within 5′ of arc, this being the limit to which settings could be made on the goniometer arcs.

Readings on the goniometer arcs could be made to 10′ with the aid of the verniers. The film was then set at 5 cm. from the crystal by making two exposures with the film holder moved through a measured distance. By measuring the distances between corresponding spots on these two films, the movement of the film holder required to place the film 5 cm. from the crystal was

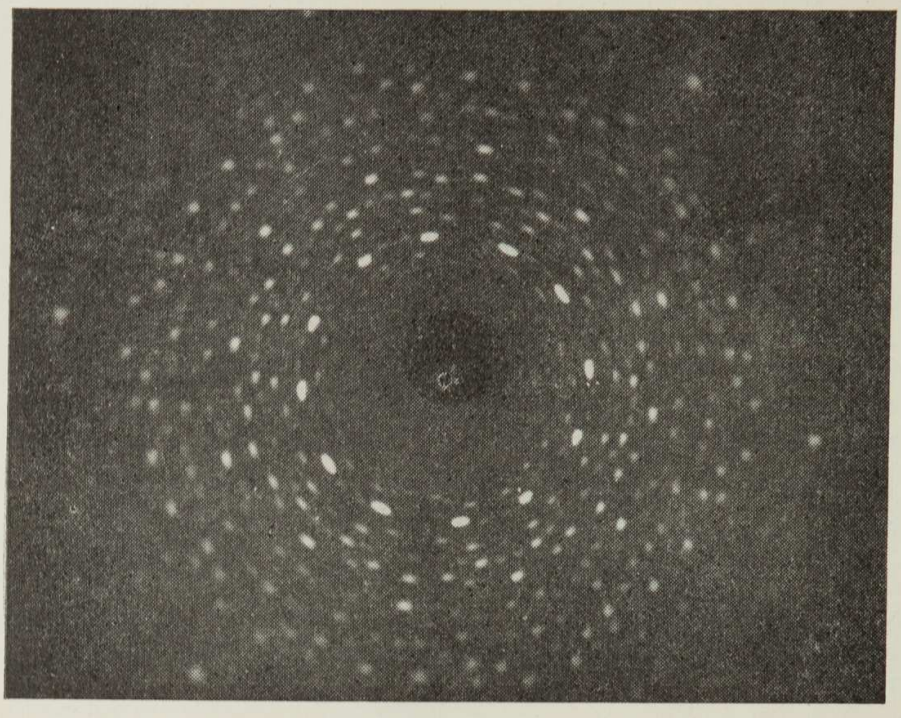

Text fig. 1.—Laue Diffraction Pattern Beryl with the X-rays travelling along the *c* axis.

calculated. All of these preliminary patterns were obtained using 1 mm. collimating pin holes to shorten exposure times. The final pattern was obtained with 0.5 mm. pin holes in the collimator. It is shown in text fig. 1 ; a slight asymmetry is detectable by accurate measurements of the diffraction spots.

The crystal was then adjusted until the line of symmetry in text fig. 1 that is inclined at 10° to the horizontal (the horizontal direction being the direction from left to right in the figure) was approximately parallel to the X-ray beam. This direction was subsequently established as being that of the *a* axis.

As with the *c* axis the final adjustments were made with the aid of exposures.

Text fig. 2 shows the resulting pattern.

Single Crystal Rotation Photographs.

To obtain these the crystal was first rotated about its *c* axis, and was irradiated with CuKα and MoKα radiations. The patterns were recorded on films placed in a cylindrical camera, the axis of the camera coinciding with the rotation axis of the crystal.

The same procedure was repeated to obtain a pattern for rotation about an *a* axis.

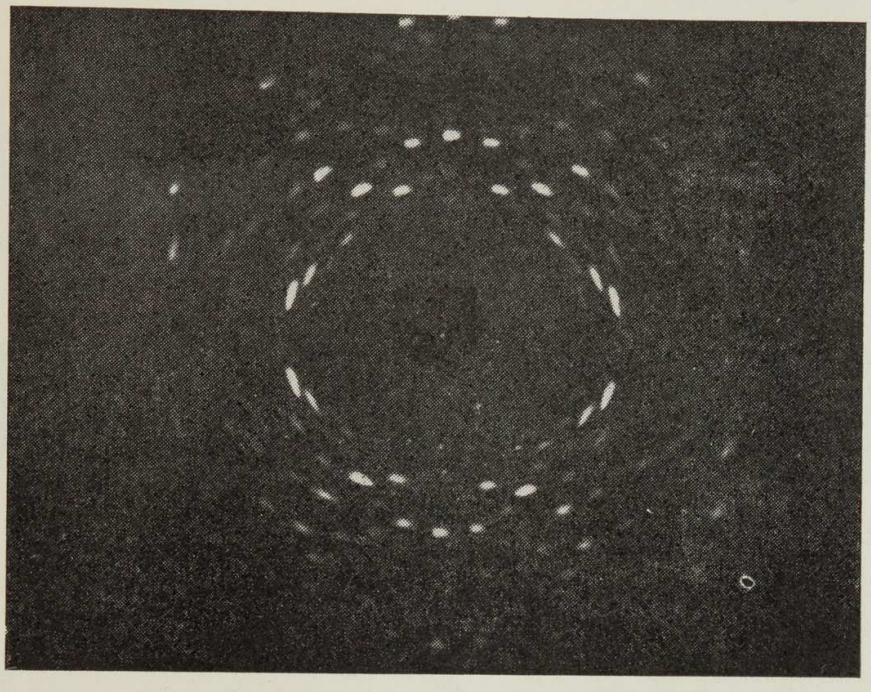

Text fig. 2.—Laue Diffraction Pattern of Beryl taken with the X-rays parallel to an *a* axis.

Text fig. 3 gives a reprint of the pattern obtained using CuKα radiation with the crystal rotated about its *c* axis.

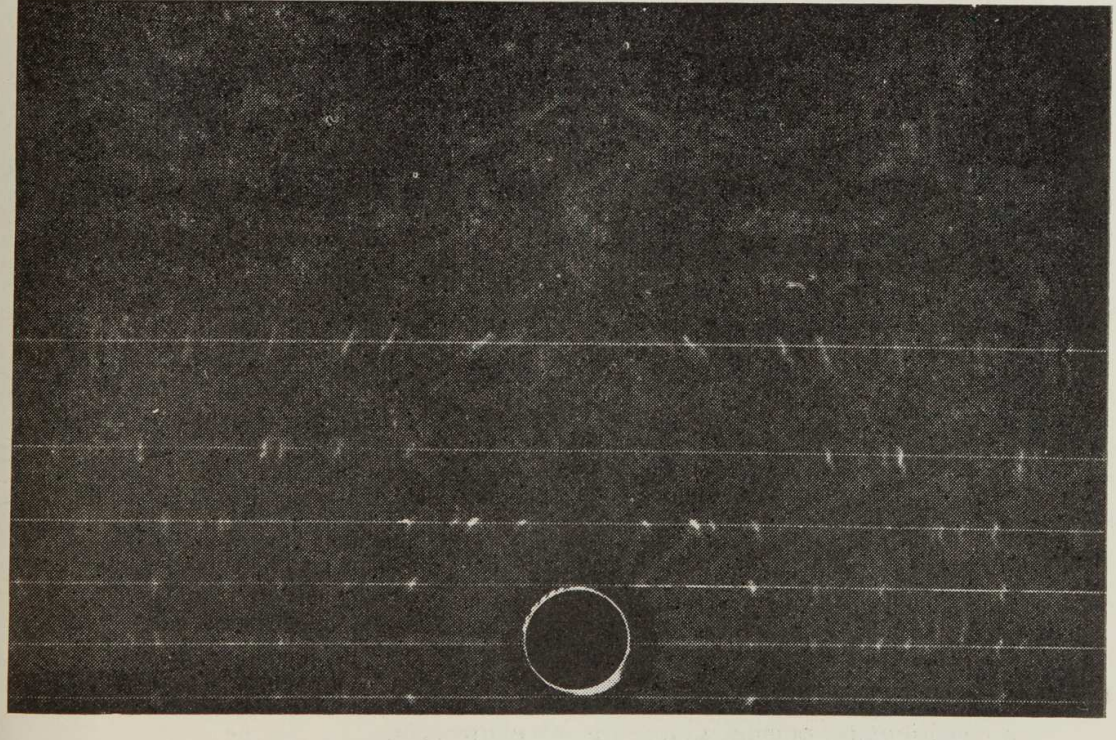

Text fig. 3.—Diffraction Pattern of Beryl rotating about its *c* axis. (The fine horizontal lines were drawn in when measuring the negative.

From the reprint it can be seen that the diffraction spots are duplicated and that the layer lines are not straight. The duplication of the diffraction spots was due to the crystal being slightly out of adjustment, that is, the

rotation axis did not coincide with the axis of the crystal. The curvature of the layer lines was the result of the axis of the camera and the rotation axis, not coinciding.

Powder Diffraction Pattern.

A small piece of beryl was powdered by crushing between two hard pieces of steel, the beryl being too hard to be ground in an agate mortar. After crushing, an electro-magnet was used to separate out any pieces of iron. The powder was sieved through a piece of fine silk and then packed into a cylindrical sample tube. The sample was mounted on the spectrograph and a diffraction pattern recorded using CuKα radiation.

Text fig. 4.—Powder Diffraction Patern of Beryl.

RESULTS AND THEIR INTERPRETATION.

Symmetry.

All symmetry data were obtained from the Laue diffraction patterns. The Laue photograph taken with X-rays parallel to the c axis exhibits a six-fold axis of rotation and six lines of reflection. The pattern taken with X-rays travelling along the a axis has a two-fold rotation axis and two lines of reflection. These symmetry elements of the Laue patterns give beryl the diffraction symmetry 6/mmm (D_6h)*. With this diffraction symmetry, beryl must lie in one of the crystal classes (*see* references (6) and (7)):

$\bar{6}$ /m 2	(D_3h)
6 m m	(C_6v)
6 2	(D_6)
6/m m m	(D_6h)

These classes all give the same diffraction symmetry because Laue photographs always exhibit a centre of symmetry, irrespective of whether the crystal under consideration possesses one or not.

Unit Cell.

(a) *Parameters.*—The demensions of the axis of the unit cell were found, approximately from the single crystal rotation photographs, and then accurately from the results of the powder diffraction pattern.

From text fig. 3 it can be seen that the diffraction spots lie along straight lines, commonly known as layer lines. The layer line containing the direct beam is the zero layer line ; that on either side of this the first order layer line and so on.

Text fig. 5 shows how the X-rays are diffracted by the rotating crystal. O and P are diffracting points, in the crystal, lying on the rotating axis.

t is the identity period along the rotation axis.

ϕ is the angle the diffracted beam makes with the horizontal.

n is the order of the layer line containing the diffraction spot.

* The internationally adopted symbols are used, but because many authors still use Schoenflies symbols, these are given in brackets.

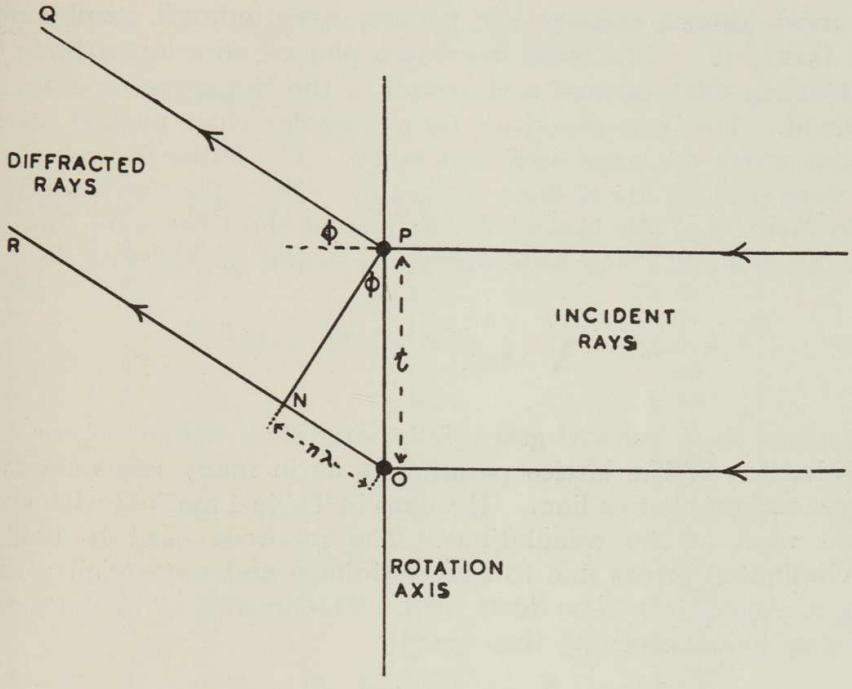

Text fig. 5.—Diffraction of X-rays by a rotating crystal.

From the geometry of the figure it is obvious that when the diffracted beams from O and P are in phase so as to produce a diffraction spot on the fiim, then $n\ \lambda = t\ \text{Sin}\ \phi$ .... (1)

λ being the wavelength of the X-rays.

If s is the distance of the nth order layer line from the zero layer line then

$$\text{Tan}\ \phi = \frac{s}{r} \quad \ldots\ \ldots\ \ldots\ (2)$$

The radius r of the camera was measured mechanically corrections being applied for the thickness of the paper envelope and film. The corrected value of the radius was 3.32 cm.

When the rotation is about an axis of the crystal, then the identity period, t, becomes the length of the axis. The results and calculations for the c axis are given in Table 3.

TABLE 3.

Rotation about c axis. CuKα radiation.

Layer Line.	s in cm.	ϕ	c in A.U.
1	0.56	9°35′	9.24
2	1.19	19°43′	9.12
3	1.92	30° 3′	9.21
4	2.99	42° 1′	9.20

Average value of c = 9.19 A.U.

The value of c calculated from a photograph taken with MoKα radiation agreed well with the aforementioned value of c.

The value of the a axis, determined in a similar manner, gave an average value of 9.20 A.U.

To calculate the axial lengths accurately the lines of the powder diffraction pattern were measured and the interplanar spacing, d/n, of each line was calculated from Bragg's equation $n\ \lambda = 2d\ \text{Sin}\ \theta$.

The most intense lines on the pattern were indexed graphically as described in Davey (8). The main lines were plotted on a logarithmic scale, the scale then being tried against each graph of the hexagonal system until a fit was obtained. This was found on the triangular close packed lattice graph at the point where the axial ratio was unity. The Miller indices of the larger spacings were read off direct from the graph. The higher orders of these lines were then indexed. The indices of the rest of the lines were found by trial and error, after a and c had been calculated, using the formula :—

$$d_{h\ k\ l} = \sqrt{\frac{4}{3a^3}(h^2 + k^2 + hk) + \frac{l^2}{c^2}} \quad \ldots\ldots \quad \ldots\ldots \quad (3)$$

Only those lines indexed graphically, and their higher orders, were used in the evaluation of the lattice parameters as in many cases several sets of indices were assignable to a line. The lines in Table 4 marked with an asterisk, were those used in the calculations. The methods used to calibrate the camera, eliminated errors due to film shrinkage and eccentricity, absorption being the only error left to be dealt with. The error $\Delta\ \theta$ in the Bragg angle due to absorption, is given by Buerger (9)

$$\Delta\ \theta = \mathrm{E}\ \mathrm{Cos}^2\ \theta.$$

where E is a constant depending on the degree of divergence of the X-ray beam. This gives (9) for the error equation

$$\left(\frac{n\ \lambda}{2\ d}\right)^2 = \mathrm{Sin}^2\theta - \mathrm{E}\ \mathrm{Cos}^2\theta\ \mathrm{Sin}\ 2\ \theta$$

which may be written

$$a\ \mathrm{D} = \mathrm{Sin}^2\theta - \varepsilon\ \mathrm{E}.$$

where $n^2 = a$, $\left(\frac{\lambda}{2d}\right)^2 = \mathrm{D}$ and $\mathrm{Sin2}\ \theta\ \mathrm{Cos}^2\theta = \varepsilon$.

The most probable value of D and therefore of d is given (9) by

$$\mathrm{D} = \begin{vmatrix} \Sigma\ a\ \mathrm{Sin}^2\theta & \Sigma\ a \\ \Sigma\ \varepsilon\ \mathrm{Sin}^2\theta & \Sigma\ \varepsilon^2 \\ \hline \Sigma\ a^2 & \Sigma\ a\ \varepsilon \\ \Sigma\ a\ \varepsilon & \Sigma\ \varepsilon^2 \end{vmatrix} \quad (4)$$

This gives the best value of the spacing, d, corrected for absorption errors. If the indices of the spacing are of the form ($h\ k$ O) or (O O l), then a *or* c may be determined directly from the application of formula (3).

For spacings whose indices are of the general form, ($h\ k\ l$) then a and c are determined by using two spacings, obtaining two equations from (3) to solve for a and c.

The calculations, using the above methods were long and laborious and are not shown here, but the values of the parameters were

$$a = 9.188\ \text{A.U.}$$
$$c = 9.189\ \text{A.U.}$$

The error in each case was certainly less than 0.01 A.U. and was probably about half of this. These results show that the chosen axis was the a axis.

TABLE 4.

Results of the Powder Diffraction Pattern.

Line.	Intensity.	$\theta°$	d/n A.U.	Miller Indices.
1	vw	5°	8.83	β of (100)
2	st	5°34′	7.93	(100)*
3	m	9°38′	4.60	(002)*
4	m	11°12′	3.96	(200)*
5	w	12°21′	3.60	β of (112)
6	st	13°42′	3.25	(112)*
7	m	14°48′	3.01	(202) (210)
8	st	15°37′	2.86	(211)*
9	vvw	16°54′	2.65	(300)*
10	m	17°51′	2.51	(212)*
11	w	19°39′	2.289	(220) (004)*
12	w	20°27′	2.203	(130) (104)
13	w	21° 3′	2.142	(213)
14	vw	22° 4′	2.048	(222) (114)
15	w–m	22°48′	1.986	(204) (400)*
16	vvw	23°36′	1.922	
17	vw	25° 0′	1.821	(230) (214)
18	w	25°33′	1.784	
19	w–m	26°22′	1.733	(140)
20	w	26°55′	1.700	(322) (411)
21	w	28°19′	1.622	(224)*
22	vw	28°58′	1.589	(500)*
23	vw	29°33′	1.561	(215) (702)
24	vw	30°15′	1.528	(330) (006)*
25	w	30°43′	1.507	(106) (404) (420)
26	w	32° 4′	1.450	(116) (332)
27	w	32°36′	1.429	(422)*
28	w	34°24′	1.362	(216)
29	vvw	35°24′	1.328	(306) (600)*
30	w–m	37°15′	1.272	(250) (226) (602)
31	w–m	37°45′	1.257	(251) (424)*
32	w–m	39°52′	1.200	(217)
33	vvw	40°54′	1.176	(523)
34	vw	42° 6′	1.148	(440) (008)*
35	vw	42°42′	1.134	(108) (700)*
36	vw	43°42′	1.114	(118) (442)
37	vvw	44°12′	1.104	(260) (208)
38	vvw	45°15	1.083	(336)*
39	vvw	45°51′	1.073	(426) (218)
40	vvw	46°15′	1.065	(353) (345)
41	vw	47°22′	1.046	(156)
42	vvw	48°30′	1.028	(444) (228)
43	vvw	49°30′	1.012	(451)
44	vvw	50° 7′	1.002	(630) (606)*
45	vw	50°39′	0.9951	(408) (800)*
46	vw	52°18′	0.9725	(270) (802)
47	vw	52°45′	0.9668	(219)
48	vw	53°30′	0.9572	(714)
49	vw	56°51′	0.9191	(550) (00, 10)*
50	vw	57°27′	0.9128	(460) (428)
51	vvw	58°42′	0.9005	(552)
52	vw	59°48′	0.8904	(813) (455)
53	vw	61° 6′	0.8790	(21, 10)
54	vvw	62°30′	0.8676	(280) (902)
55	vw	64°24′	0.8533	(22, 10)
56	vw	67°15′	0.8345	(636)*
57	vw	67°39′	0.8320	

* Lines used in determining lattice parameters.

N.B.—All the indices are expressed in the form (h k l). It has been a general practice with the hexagonal system to give the indices (h k i l) but as $i = h + k$, the author considered that the indices (h k l) were sufficient. h and k are interchangeable.

st = strong, m = medium, w = weak, v = very.

(b) *Number of Molecules per Unit Cell.*—Knowing the density of beryl, the weight of a molecule, and the volume of the unit cell, the number of molecules in a unit cell can be calculated.

The volume of a unit cell in the hexagonal system is

$$V = a^2 c \sin 60 \tag{5}$$

The density of beryl is given by

$$\rho = \frac{m\ M}{V} \tag{6}$$

where m is the number of molecules per unit cell and M is the mass of a molecule expressed in grams.

Combining (5) and (6) we have

$$m = \frac{a^2\ c\ \text{Sin } 60}{M} \tag{7}$$

The experimental values of ρ, a and c and the value of M (table 2) reduced to grams, were used in (7) to give

$$m = 2.05.$$

Since the number of molecules in a unit cell must be integral, there are two molecules per unit cell.

Another way of viewing the above result is that, assuming two molecules per unit cell, the density calculated from X-ray data is 2.64 gm. cm.$^{-3}$. This agrees reasonably well with the experimental density. (Even with chemicals and elements of high purity, the discrepancies between the calculated and experimental densities are large.)

(c) *Confirmation of the Unit Cell.*—Because Laue diffraction patterns contain reflections from many planes, they are used to see if the chosen unit cell accounts for the observed reflections. Each set of planes in the crystal diffracts that wavelength in the X-ray beam that satisfies Bragg's Law. When the position of the crystal axes is known with respect to the X-ray beam, as in the present cases, then it is possible by calculation to find the Miller indices of the planes responsible for each diffraction spot.

The angle, θ, at which the X-ray beam meets the diffracting planes, is the sole factor governing the position of the diffraction spot (situated at 2θ) on the film. This means that the various orders of a particular spacing will all be super-imposed and that the resultant diffraction spot will be contributed to by several different wavelengths.

To index all the spots on Laue film, analytically, would be a tedious process so that the indexing was performed graphically by the gnomonic projection method. A gnomonic projection rule was made, as described in Wyckoff (10), from celluloid. The theory of gnomonic projection is shown in text fig. 6. X-rays strike the extended crystal plane RSTU at an angle θ. The direct beam registers on the film MNOP at C′ and the diffracted beam at F′. The gnomonic projection of the reflecting plane is G where GC is perpendicular to the plane RSTU. From the geometry of the figure it is seen that

$$GC' = CC' \text{ Cot } \theta \tag{8}$$

$$F'C' = CC' \text{ Tan } 2\theta \tag{9}$$

The distance of the film from the crystal, CC′, was 5 cm., so that

$$GC' = 5 \text{ Cot } \theta \text{ and } F'C' = 5 \text{ Tan } 2\theta.$$

If the point F′ is known it is possible to calculate the corresponding point G. The process is carried out graphically with the aid of a gnomonic projection rule, one side of which measures the distance C′F′ (the distance of the diffraction spot from the direct beam) while the other side is graduated in accordance with the requirements of equations (8) and (9) to give the projected distance GC′.

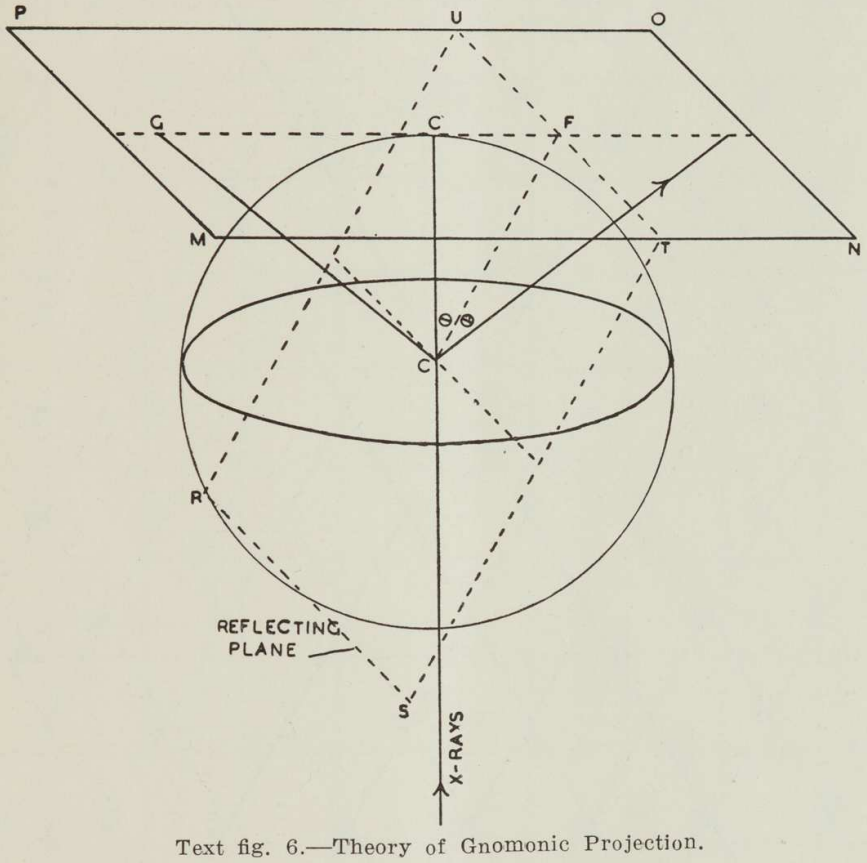

Text fig. 6.—Theory of Gnomonic Projection.

To carry out the gnomonic projection a co-ordinate system, see text fig. 7, was first drawn. For the Laue film with X-rays travelling parallel to the *c* axis, this consisted of two sets of parallel lines inclined at 60°, that is, the unit of the network was a rhomb with a 60° angle. It is easily demonstrated that the side of a rhomb is equal to

$$\frac{CC'}{\text{Cos } 30} \times \frac{c}{a}$$

giving 5.77 cm. for the case under consideration. The Laue photograph was placed on the network with the spot due to the direct beam at the intersection of two lines and with two of the *a* axes lying along these lines. The ruler was placed with its zero over the direct beam and the projection was carried out. This procedure was rapid and free from errors. The projected points lay on the corners of rhombs or simple submultiples of them. The Miller indices were read off direct from the chart, all the indices having $l = 1$.

In text fig. 7, for clearness, only a few of the spots are shown plotted.

The simplest method of judging whether the assumed unit cell accounts for the observed reflections is to compare the observed and predicted intensities of the Laue spots.

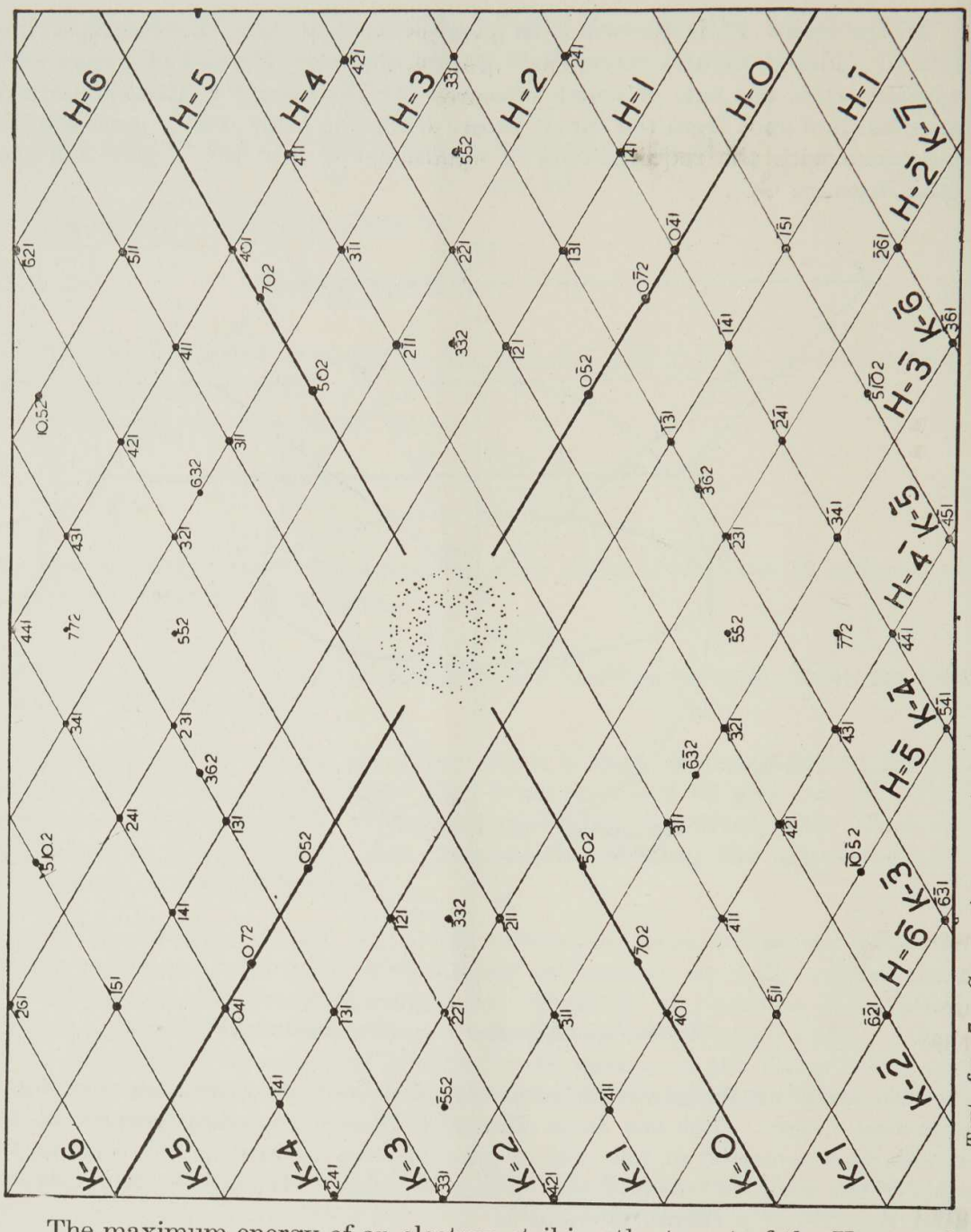

Text fig. 7.—Gnomonic projection of a Laue photograph of Beryl, X-rays travelling to c axis.

The maximum energy of an electron striking the target of the X-ray tube is

$$E_{max} = e\,V = h\,\nu = \frac{h\,c}{\lambda_{min}} \qquad (10)$$

e is the charge on the electron,
V is the potential difference between the electrodes of the X-ray tube,
h is Planck's constant,
ν is the maximum frequency of the X-rays,
λ_{min} is the minimum wavelength present,
c is the velocity of light.

For an applied voltage of 60 kilovolts we have

$$\lambda_{min} = \frac{h\,c}{e\,V} = 0.21 \text{ A.U.} \qquad (11)$$

Text fig. 8 shows a graph obtained by plotting wavelength against the blackening effect on the film. No radiation is present with a wavelength of less than 0.21 A.U. but its intensity rises rapidly from 0.21 A.U. to reach a maximum at approximately $2\lambda_{min}$ (0.48 A.U.). The discontinuity at 0.48 A.U. is due to the critical absorption edge of silver being at 0.48 A.U. The bromine in the film emulsion causes the other discontinuity in the curve at 0.92 A.U.

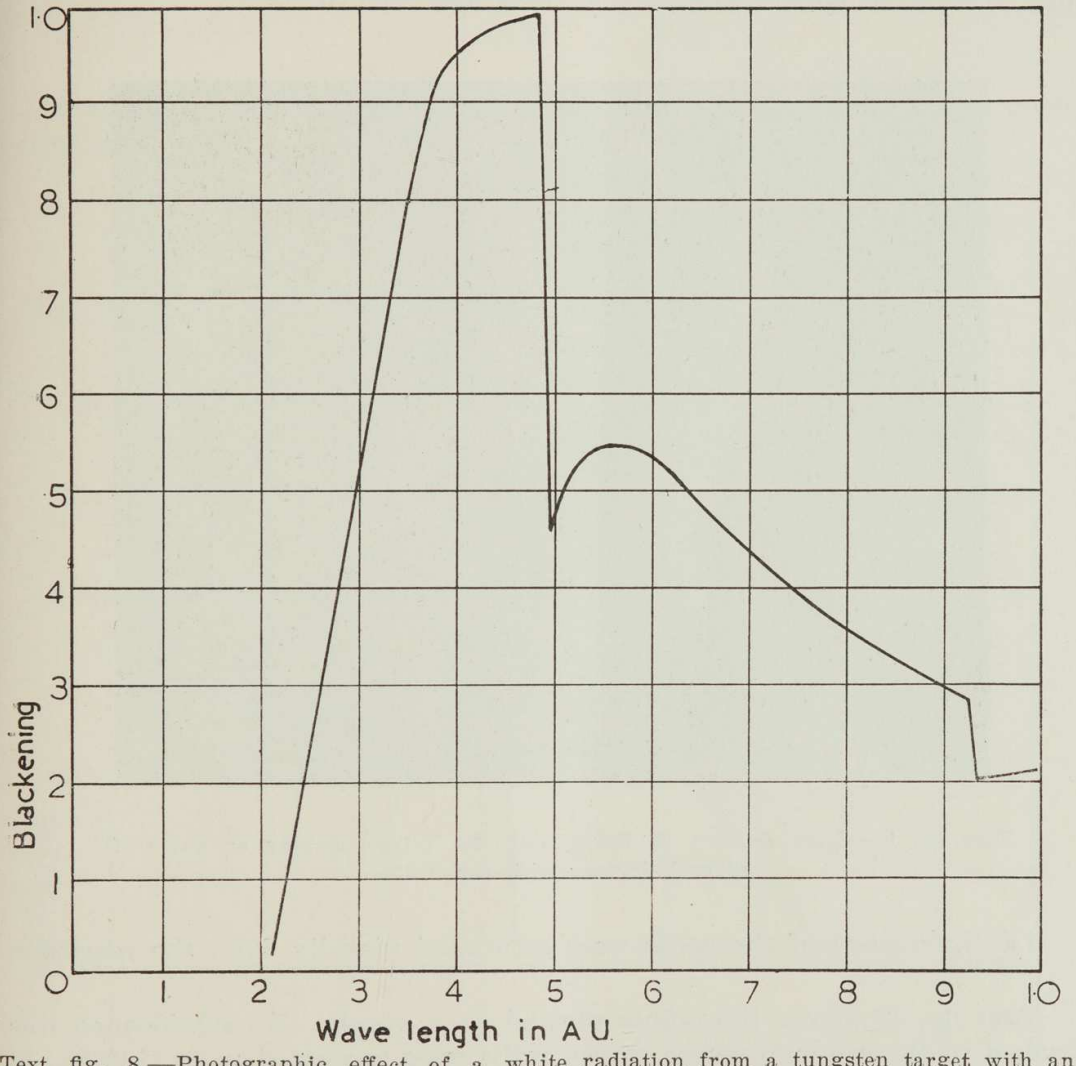

Text fig. 8.—Photographic effect of a white radiation from a tungsten target with an applied voltage of 60 Kilovolts.

By applying Bragg's Law to a diffraction spot whose Miller indices are known, the wavelength producing the spot may be calculated ; d/n is calculated from the crystal parameters using equation (3) and θ is determined from the distance of the spot from the direct beam. This applies only to those wavelengths between λ_{min} and $2\lambda_{min}$, that is, between 0.21 and 0.42 A.U. Spots, due to fundamental spacings, and wavelengths of less than $2\lambda_{min}$, are the result of one wavelength only as there is no wavelength present that is short enough to be diffracted by the higher orders of the spacing. Spots with $n\lambda > 2\lambda_{min}$ may be contributed to by several different wavelengths due to higher orders.

In plotting a graph of wavelength against blackening on the film, only planes of the one form (that is, planes with the same diffracting power) may be used. On a Laue photograph with X-rays travelling parallel to an axis,

all the spots due to planes of the same form have the same θ and consequently are due to the same wavelength. In this case, the various spots would be coincident on a graph. To obtain a photograph in which the diffraction spots, due to planes of the one form, have different θ's, an exposure was made with the X-rays making an angle of several degrees with the c axis. This Laue photograph is shown in text fig. 9 ; it was taken during the setting of the crystal. The spots on this pattern were indexed by a visual comparison with those of text fig. 1, whose diffraction spots had been indexed.

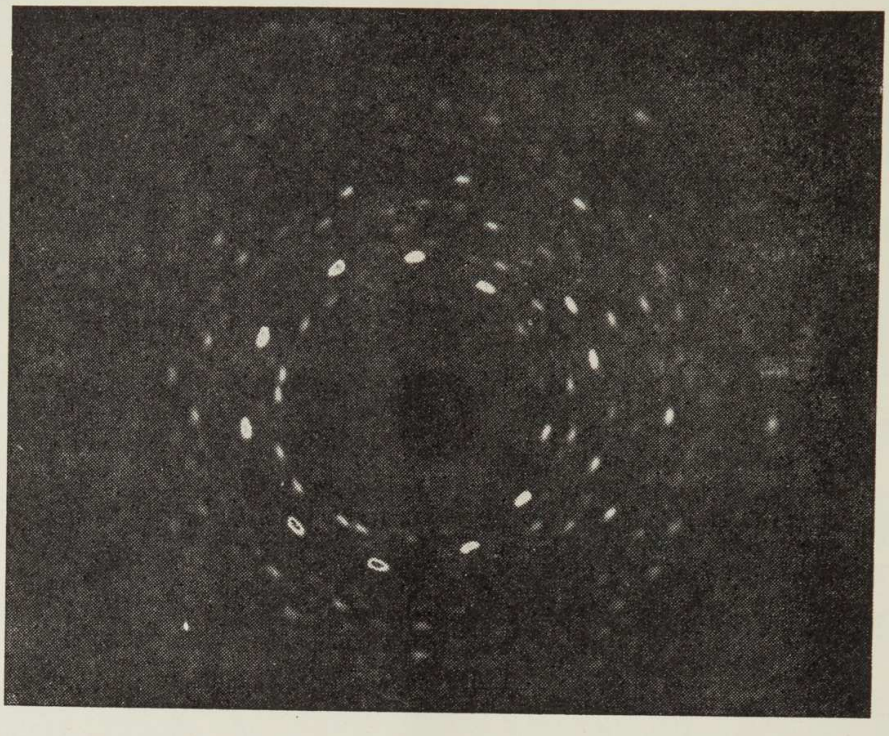

Text fig. 9.—Laue Pattern of Beryl with the X-rays making an angle of several degrees with the c axis.

The intensities of the spots were estimated visually from the negative.

Text fig. 10 shows the points plotted on a graph. No significance was attached to those points whose wavelengths were greater than 0.44 A.U., in confirming the unit cell. The curve shows the correct minimum and maximum wavelengths with the silver absorption edge at the correct position.

Space Group.

Standard treatises on crystallography place beryl in the holosymmetric class of the hexagonal system (6/mmm). This is in agreement with the data given earlier in the section on Symmetry.

A study of the spacings present and absent on the powder diffraction pattern, shows the absence of the following classes of reflection, (h 0 l) and (h h l) in cases where l is odd. The extinction of the (h h l), l odd, reflections indicates a (1 $\bar{1}$ 0) glide plane of component $c/2$; the extinction of the (h 0 l), l odd, reflections implies a (0 1 0) glide plane of component $c/2$ (11). The diffraction symbol for beryl now becomes 6/mmm C/cc. Knowing that beryl belongs to the crystal class 6/mmm, the space group is C6/mcc (D_6^2h) (12).

No attempt was made to place the atoms of beryl within the unit cell.

Bragg and West (13) have made a complete analysis of the structure of beryl. All of the above results are in accord with their conclusions. They give the lengths of the crystal axis as

$$c = 9.17 \pm 0.01 \text{ A.U.}$$

and

$$a = 9.21 \pm 0.01 \text{ A.U.}$$

The variation in the lattice parameters is probably due to the impurities contained in beryl.

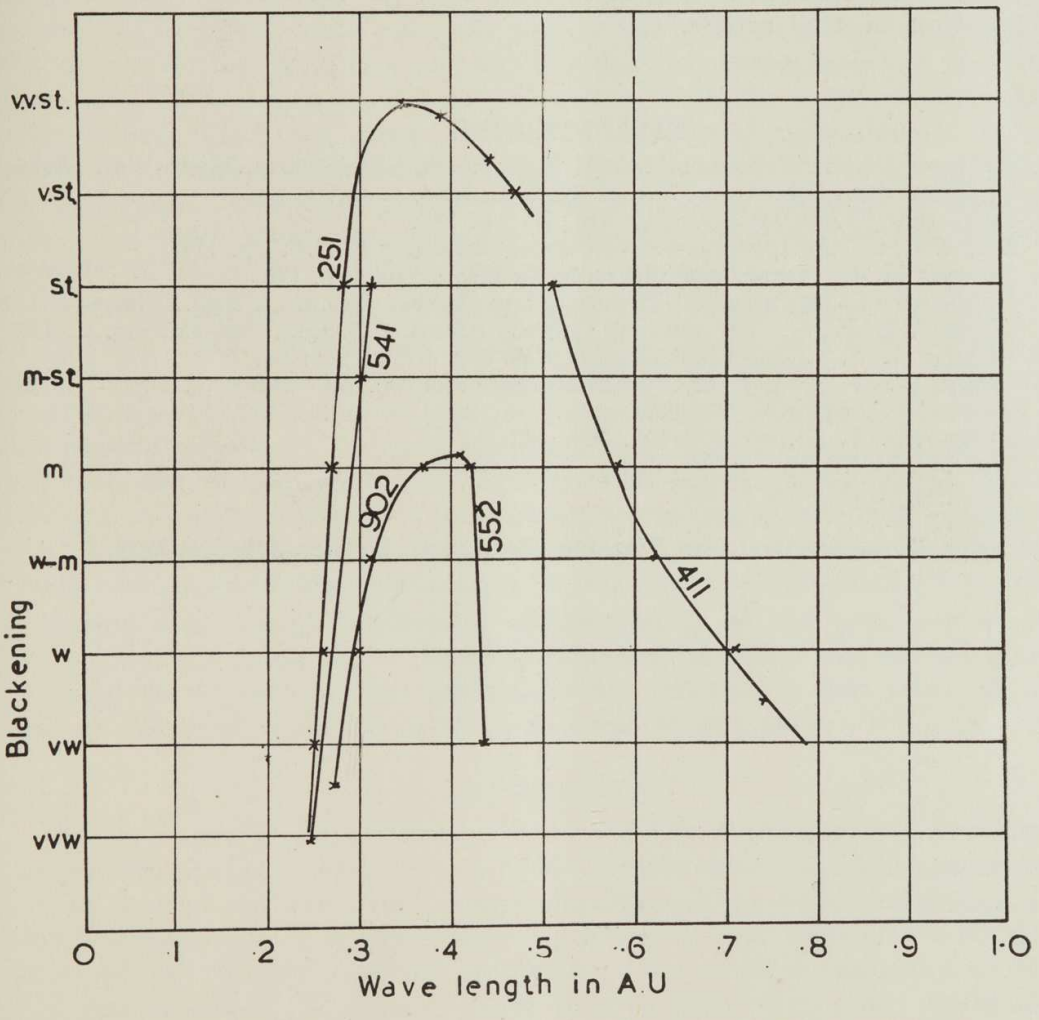

Text fig. 10.—Experimental curve showing the blackening effect of X-rays.

SUMMARY.

The Laue, the single crystal rotation and the powder methods of X-ray analysis were used to study a crystal of Western Australian beryl. The techniques and methods of interpretation, associated with the different methods, are described.

The results obtained are in agreement with the other published data on beryl.

ACKNOWLEDGMENTS.

The studies were carried out in the Physics Department of the University of Western Australia during the tenure of a Hackett Research Scholarship and a Commonwealth Research grant. The author wishes to thank the University of Western Australia for the former and the Council for Scientific and Industrial Research for the latter.

Dr. R. T. Prider of the Department of Geology of the University and Dr. D. Carroll of the Government Chemical Laboratories suggested the work and the author is indebted to them for supplying the samples together with optical and chemical data on beryl.

Mr. J. Shearer of the Department of Physics of the University of Western Australia supervised the work and the author is grateful to him for his guidance and assistance in the experimental work and for his advice concerning the preparation of this article.

BIBLIOGRAPHY.

(1) Matheson, R. S. Report on M.C.291 H for Beryl, Yinnietharra, North-West Division. (From *Ann. Report, Geo. Sur. of W.Aust.*, 1944, p. 42.)
(2) Dictionary of Applied Physics. Vol. III., p. 132.
(3) Evans, R. C. An Introduction to Crystal Chemistry (C.U.P.), p. 171.
(4) Buerger, M. J. X-ray Crystallography (Wiley & Sons), p. 179.
(5) Handbook of Chemistry and Physics (Chem. Rubber Pub. Co.), 28th Edition, p. 1926.
(6) Wyckoff, R. W. G. Structure of Crystals (Chem. Cat. Co.), 2nd Edition, p. 127.
(7) Buerger, M. J. X-ray Crystallography (Wiley & Sons), p. 84.
(8) Davey, W. P. A Study of Crystal Structure and its Applications (McGraw-Hill Book Co. Inc.), pp. 128, 596-602.
(9) Buerger, M. J. (7), pp. 402–407, 428, 432.
(10) Wyckoff, R. W. G. (6) pp. 131.
(11) Buerger, M. J. (7), p 83.
(12) Buerger, M. J. (7). p. 514.
(13) Bragg, W. L. and West, J. *Proc. Roy. Soc., Lond.* III. (A), 691–714, 1926.

By Authority: WILLIAM H. WYATT, Government Printer, Perth.